

Probing heavy triplet leptons of the type-III seesaw mechanism at future muon colliders

Tong Li,^{1,*} Han Qin,^{2,†} Chang-Yuan Yao,^{1,3,‡} and Man Yuan^{1,§}

¹*School of Physics, Nankai University, Tianjin 300071, China*

²*PITT PACC, Department of Physics and Astronomy,
University of Pittsburgh, Pittsburgh, PA 15217, USA*

³*Deutsches Elektronen-Synchrotron DESY,
Notkestraße 85, 22607 Hamburg, Germany*

Abstract

We study the search potential of heavy triplet leptons in Type III Seesaw mechanism at future high-energy and high-luminosity muon colliders. The impact of up-to-date neutrino oscillation results is taken into account on neutrino parameters and the consequent decay patterns of heavy leptons in Type III Seesaw. The three heavy leptons in the Casas-Ibarra parametrization with diagonal unity matrix are distinguishable in their decay modes. We consider the pair production of charged triplet leptons E^+E^- through both $\mu^+\mu^-$ annihilation and vector boson fusion (VBF) processes. The leading-order framework of electroweak parton distribution functions are utilized to calculate the VBF cross sections. The charged triplet leptons can be probed for masses above ~ 1 TeV. The $E^+E^- \rightarrow ZZ\ell^+\ell^-$ channel can be further utilized to fully reconstruct the three triplet leptons and distinguish neutrino mass patterns. The pair production of heavy neutrinos N and the associated production $E^\pm N$ are only induced by VBF processes and lead to lepton-number-violating (LNV) signature. We also study the search potential of LNV processes at future high-energy muon collider with $\sqrt{s} = 30$ TeV.

* litong@nankai.edu.cn

† han.qin@pitt.edu

‡ yaocy@nankai.edu.cn

§ yuanman@mail.nankai.edu.cn

I. INTRODUCTION

Neutrino oscillation experiments have provided compelling evidence that neutrinos have small but finite masses. It is well-known that, in the context of the Standard Model (SM), the small Majorana neutrino masses can be generated at leading order through a dimension-5 “Weinberg operator” [1]

$$\frac{\kappa}{\Lambda} LLHH, \quad (1)$$

where L and H stand for the SM left-handed lepton doublet and the Higgs doublet, respectively. The ultraviolet completions of Eq. (1) at tree level [2] are only implemented by the Type I [3–9], Type II [9–13] and Type III [14] Seesaw mechanisms. As proved in Refs. [15, 16], requiring all three light neutrinos to be massless is equivalent to requiring lepton number to be conserved at all orders in perturbation theory. In other words, in light of non-zero neutrino masses, lepton number is nearly conserved in low-scale seesaw models with fermionic singlets. Thus, for low-scale Type I Seesaw, the observable lepton number violation (LNV) is decoupled in high energy processes. Any observation of lepton number violation at high-energy colliders implies an extension of the canonical Type I Seesaw. In particular, the Type III Seesaw introduces at least two $SU(2)_L$ triplet lepton representations Σ_L with $(1, 3, 0)$ SM quantum numbers. The active neutrino mass matrix has the same form as that in Type I Seesaw and the high energy scale Λ is given by integrating out the mass of triplet leptons which can be as low as a few TeV.

On the other hand, several reactor experiments have provided precise measurements for the neutrino mixing parameters. For instance, Double Chooz [17], RENO [18] and in particular Daya Bay [19] have reported non-zero measurements of θ_{13} by looking for the disappearance of anti-electron neutrino. More recently, two long-baseline neutrino experiments T2K [20] and NOvA [21] reported the indication of a non-zero CP-violating phase. Despite a slight tension at $\sim 2\sigma$ level between them, these experiments provide us up-to-date neutrino oscillation results to investigate the impact on neutrino mass models. As the sign of the mass-squared difference Δm_{31}^2 has not been determined up to now, the so-called normal hierarchy (NH) with positive Δm_{31}^2 and the inverted hierarchy (IH) with negative Δm_{31}^2 are normally considered in the data analysis. Future neutrino oscillation experiments, such as T2HK [22], JUNO [23] and DUNE [24], are very likely to further explain the discrepancy and make a distinction between these two neutrino mass patterns. Besides the neutrino experiments, high-energy colliders can also provide complementary strategies to reveal the neutrino properties by searching for the triplet leptons and leptonic signatures.

The new triplet leptons in TeV Type III Seesaw mechanism can be experimentally accessible at the Large Hadron Collider (LHC) (see Refs. [25–35] and the references therein) and lepton colliders [36–39]. The triplet leptons are produced in pairs through pure electroweak (EW) gauge couplings and followed by multi-lepton signatures. After combining two-, three- and four-lepton channels together, the observed lower limit on the mass of heavy leptons is above 900 GeV at the 95% confidence level (CL) [40, 41]. According to the theoretical estimations, it is difficult to

discover the lepton-number-conserving or lepton-number-violating signal events for triplet leptons heavier than ~ 1 TeV at the LHC. One needs a bigger machine with higher energy and integrated luminosity. Recently, high energy muon colliders have received much attention in the community due to the technological developments [42–44]. The community considers the high-energy option of muon collider with multi-TeV center-of-mass (c.m.) energies and a high integrated luminosity scaling with energy quadratically [43]

$$\mathcal{L} = \left(\frac{\sqrt{s}}{10 \text{ TeV}} \right)^2 10 \text{ ab}^{-1} . \quad (2)$$

It thus provides excellent opportunities to produce and discover new heavy EW particles such as the triplet leptons in Type III Seesaw.

In this work, we investigate the search for heavy triplet leptons at high-energy muon colliders. The pair productions of heavy triplet leptons are categorized into the topologies of direct $\mu^+\mu^-$ annihilation and the vector boson fusion (VBF). The mass eigenstates of charged triplet lepton (denoted by E^\pm) can be produced in pairs through both of these two processes. The large total cross section of E^+E^- production makes it an appealing discovery channel of the triplet lepton. By contrast, the associated production of E^\pm and the neutral heavy neutrino N as well as the pair production of N are only induced by VBF processes. In spite of their small production cross sections, they can produce distinctively rare LNV signal and play as crucial channels to determine Majorana neutrino property and distinguish triplet mass eigenstates at high energies.

This paper is organized as follows. In Sec. II, we first outline the Type III Seesaw model and discuss the constraints from neutrino oscillation experiments on the decay patterns of heavy triplet leptons. Then we simulate the pair production of heavy triplet leptons via $\mu^+\mu^-$ annihilation and VBF at high-energy muon colliders in Sec. III. The results of projected sensitivity for heavy leptons are also given. Finally, in Sec. IV we summarize our conclusions.

II. TYPE III SEESAW AND HEAVY TRIPLET LEPTONS

In addition to the SM fields, the Type III Seesaw [14] consists of $\text{SU}(2)_L$ triplet leptons with zero hypercharge, i.e., $\Sigma_L \sim (1, 3, 0)$ under SM gauge group $\text{SU}(3)_C \times \text{SU}(2)_L \times \text{U}(1)_Y$:

$$\Sigma_L = \begin{pmatrix} \Sigma_L^0/\sqrt{2} & \Sigma_L^+ \\ \Sigma_L^- & -\Sigma_L^0/\sqrt{2} \end{pmatrix} . \quad (3)$$

The Type III Seesaw Lagrangian is given by the kinetic term, mass term and Yukawa interactions in terms of Σ_L and its charge conjugated form Σ_L^c

$$\mathcal{L}_T = \text{Tr} [\bar{\Sigma}_L i \not{D} \Sigma_L] - \left(\frac{1}{2} \text{Tr} [\bar{\Sigma}_L^c M_\Sigma \Sigma_L] + Y_\Sigma \bar{l}_L \tilde{H} \Sigma_L^c + \text{H.c.} \right) , \quad (4)$$

where $\tilde{H} = i\sigma_2 H^* \sim (1, 2, -1)$. Besides the neutrino mass mixing for $(\nu_L, \Sigma_L^0)^T$, the Yukawa term in Eq. (4) also induces a mass mixing between the charged SM leptons and the charged triplet

leptons

$$\begin{pmatrix} \overline{\nu}_L^c & \overline{\Sigma}_L^{0c} \end{pmatrix} \begin{pmatrix} 0 & Y_\Sigma^T v_0/2\sqrt{2} \\ Y_\Sigma v_0/2\sqrt{2} & M_\Sigma/2 \end{pmatrix} \begin{pmatrix} \nu_L \\ \Sigma_L^0 \end{pmatrix} + \begin{pmatrix} \overline{l}_R & \overline{\Sigma}_L^{+c} \end{pmatrix} \begin{pmatrix} m_l & 0 \\ Y_\Sigma v_0 & M_\Sigma \end{pmatrix} \begin{pmatrix} l_L \\ \Sigma_L^- \end{pmatrix} + \text{H.c.} , \quad (5)$$

where $v_0 \approx 246$ GeV is the vacuum expectation value of Higgs. After introducing unitary matrices to transit light doublet and heavy triplet lepton fields, one obtains the diagonal mass matrices and mass eigenvalues for neutrinos and charged leptons. The mass eigenstates of heavy neutral and charged leptons are denoted by N and E^\pm , respectively. Expanding the unitary matrices to leading order in $Y_\Sigma v_0 M_\Sigma^{-1}$, the mixing between the SM charged leptons and triplet lepton mass eigenstates is governed by $V_{\ell N} = -Y_\Sigma^\dagger v_0 M_\Sigma^{-1}/\sqrt{2}$. In the mass basis, to the leading order, we have the following interactions involving heavy triplet leptons

$$\begin{aligned} \mathcal{L}_{\text{Type III}} = & e \overline{E} \gamma^\mu E A_\mu + g \cos \theta_W \overline{E} \gamma^\mu E Z_\mu \\ & + \frac{g}{2 \cos \theta_W} \left[\overline{\nu}_\ell (V_{PMNS}^\dagger V_{\ell N} \gamma^\mu P_L - V_{PMNS}^T V_{\ell N}^* \gamma^\mu P_R) N + \sqrt{2} \overline{\ell} V_{\ell N} \gamma^\mu P_L E \right] Z_\mu \\ & - g \left[\overline{E} \gamma^\mu N + \frac{1}{\sqrt{2}} \overline{\ell} V_{\ell N} \gamma^\mu P_L N + \overline{E} V_{\ell N}^T V_{PMNS}^* \gamma^\mu P_R \nu_\ell \right] W_\mu^- \\ & + \frac{g}{2 M_W} \left[\overline{\nu}_\ell (V_{PMNS}^\dagger V_{\ell N} M_N^{diag} P_R + V_{PMNS}^T V_{\ell N}^* M_N^{diag} P_L) N + \sqrt{2} \overline{\ell} V_{\ell N} M_E^{diag} P_R E \right] h + \text{H.c.} , \end{aligned} \quad (6)$$

where all fields are mass eigenstates.

The above gauge interactions between SM leptons and heavy triplet leptons are all given by $V_{\ell N}$ [26, 45] and the partial widths of both heavy charged lepton and heavy neutrino are proportional to $|V_{\ell N}|^2$. In the limit of $M_E \approx M_N \gg M_W, M_Z, M_h$, the partial widths become [45, 46]

$$\begin{aligned} & \frac{1}{2} \Gamma(N \rightarrow \sum_\ell \ell^+ W^- + \ell^- W^+) \approx \Gamma(N \rightarrow \sum_\nu \nu Z + \bar{\nu} Z) \approx \Gamma(N \rightarrow \sum_\nu \nu h + \bar{\nu} h) \\ & \approx \frac{1}{2} \Gamma(E^\pm \rightarrow \sum_\nu \binom{(-)}{\nu} W^\pm) \approx \Gamma(E^\pm \rightarrow \sum_\ell \ell^\pm Z) \approx \Gamma(E^\pm \rightarrow \sum_\ell \ell^\pm h) \\ & \approx \frac{G_F}{8\sqrt{2}\pi} \sum_\ell |V_{\ell N}|^2 M_\Sigma^3 . \end{aligned} \quad (7)$$

Thus, the decay branching ratios of heavy leptons exhibit asymptotic behavior consistent with the Goldstone Equivalence Theorem [47, 48], and are given by the following relations [25, 45, 46, 49]

$$\begin{aligned} & \frac{1}{2} \text{BR}(N \rightarrow \sum_\ell \ell^+ W^- + \ell^- W^+) \approx \text{BR}(N \rightarrow \sum_\nu \nu Z + \bar{\nu} Z) \approx \text{BR}(N \rightarrow \sum_\nu \nu h + \bar{\nu} h) \\ & \approx \frac{1}{2} \text{BR}(E^\pm \rightarrow \sum_\nu \binom{(-)}{\nu} W^\pm) \approx \text{BR}(E^\pm \rightarrow \sum_\ell \ell^\pm Z) \approx \text{BR}(E^\pm \rightarrow \sum_\ell \ell^\pm h) \approx \frac{1}{4} . \end{aligned} \quad (8)$$

As the triplet mass grows, this asymptotic behavior can be seen explicitly in the triplet lepton partial widths.

There is a relation between diagonalized neutrino mass matrices and mixing matrices

$$U_{\text{PMNS}}^* m_\nu^{\text{diag}} U_{\text{PMNS}}^\dagger + V_{\ell N}^* M_N^{\text{diag}} V_{\ell N}^\dagger = 0, \quad (9)$$

with mass eigenvalues being $m_\nu^{\text{diag}} = (m_1, m_2, m_3)$ and $M_N^{\text{diag}} = (M_{N_1}, M_{N_2}, M_{N_3})$. Here the masses and mixing of the light neutrinos in the first term are measurable from the neutrino oscillation experiments. The second term contains the masses and mixing of the new heavy neutrinos. The general solution of the $V_{\ell N}$ in Eq. (9) can be parameterized in terms of an arbitrary orthogonal complex matrix Ω in the Casas-Ibarra parametrization [50]

$$V_{\ell N} = U_{\text{PMNS}} (m_\nu^{\text{diag}})^{1/2} \Omega (M_N^{\text{diag}})^{-1/2}, \quad (10)$$

with the orthogonality condition $\Omega \Omega^T = I$. Using the SM electroweak current for heavy Majorana neutrinos N_i , in the mixed mass-flavor basis, one can obtain the partial width of their decay into charged lepton [51]

$$\Gamma(N_i \rightarrow \ell^\pm W^\mp) = \frac{G_F}{8\sqrt{2}\pi} |V_{\ell N_i}|^2 M_{N_i} (M_{N_i}^2 + 2M_W^2) \left(1 - \frac{M_W^2}{M_{N_i}^2}\right)^2, \quad (11)$$

where $\ell = e, \mu, \tau$. Note that generally the Dirac mass matrix can be quite arbitrary with three complex angles parameterizing the orthogonal matrix Ω [32, 52–54]. The above asymptotic behavior of decay branching ratios of heavy neutrino indicates $\text{BR}(N_i \rightarrow \sum_\ell \ell^\pm W^\mp)$ is nearly equal to 25% for any heavy neutrino N_i ($i = 1, 2, 3$). The branching fraction of each heavy neutrino N_i decaying into any charged lepton flavor is thus less than 25% for any possible Ω matrix. In one simple case for Ω , i.e., a diagonal unity matrix $\Omega = I$, the values of $|V_{\ell N}|^2$ for each N_i are proportional to one and only one light neutrino mass [52]. The branching ratio of $N_i \rightarrow \ell^\pm W^\mp$ for any charged lepton flavor is thus independent of active neutrino mass. This representative choice of $\Omega = I$ can also lead to different leading decay into charged lepton flavor for each heavy neutrino, so one can distinguish different heavy neutrinos [54, 55]. Thus, to reduce the parameter dependence and obtain certain predictions, we take this illustrative case of Casas-Ibarra parametrization with $\Omega = I$ in the following study. Note that our results below depend on this specific case and a different choice of Ω would lead to different conclusions for individual N_i .

In order to consider the implication of the neutrino experiments, we then discuss the neutrino mass and mixing parameters in light of oscillation data. The neutrino mixing matrix can be parameterized as

$$U_{\text{PMNS}} = \begin{pmatrix} c_{12}c_{13} & c_{13}s_{12} & e^{-i\delta}s_{13} \\ -c_{12}s_{13}s_{23}e^{i\delta} - c_{23}s_{12} & c_{12}c_{23} - e^{i\delta}s_{12}s_{13}s_{23} & c_{13}s_{23} \\ s_{12}s_{23} - e^{i\delta}c_{12}c_{23}s_{13} & -c_{23}s_{12}s_{13}e^{i\delta} - c_{12}s_{23} & c_{13}c_{23} \end{pmatrix} \times \text{diag}(e^{i\Phi_1/2}, 1, e^{i\Phi_2/2}), \quad (12)$$

where $s_{ij} \equiv \sin \theta_{ij}$, $c_{ij} \equiv \cos \theta_{ij}$, $0 \leq \theta_{ij} \leq \pi/2$ and $0 \leq \delta, \Phi_i \leq 2\pi$ with δ being the Dirac CP phase and Φ_i are the Majorana phases. Taking into account the atmospheric neutrino data from

$\text{BR}(N_i)$	$e^\pm W^\mp$	$\mu^\pm W^\mp$	$\tau^\pm W^\mp$
N_1	17% (17%)	3.26% (3.73%)	4.74% (4.27%)
N_2	7.43% (7.43%)	10.75% (7.34%)	6.82% (10.23%)
N_3	0.56% (0.56%)	11% (13.93%)	13.44% (10.51%)

TABLE I. Benchmark decay branching ratios of N_i in $\Omega = I$ case for NH (IH). Here we assume the smallest light neutrino mass as 10^{-4} eV and $M_{N_i} \gg M_W$.

the Super-Kamiokande collaboration, the latest best global fit results of the neutrino masses and mixing parameters are given by [56, 57]

$$\begin{aligned}
\Delta m_{21}^2 &= 7.42 \times 10^{-5} \text{ eV}^2, \\
\Delta m_{31}^2 &= 2.510 \times 10^{-3} \text{ eV}^2 \quad (\Delta m_{32}^2 = -2.490 \times 10^{-3} \text{ eV}^2), \\
\sin^2 \theta_{12} &= 0.304, \quad \sin^2 \theta_{23} = 0.450 \text{ (0.570)}, \\
\sin^2 \theta_{13} &= 0.02246 \text{ (0.02241)}, \quad \delta_{\text{CP}} = 230^\circ \text{ (278}^\circ),
\end{aligned} \tag{13}$$

for the spectrum of the neutrino masses of NH (IH). In addition, the sum of neutrino masses is constrained to be $\sum_{i=1}^3 m_i < 0.12$ eV by combining the Planck, lensing and baryon acoustic oscillation data [58] at 95% CL. By inputting the above experimental constraints to the mixing matrix $V_{\ell N}$ and the above partial decay width formulas, we can obtain the preferred values of decay branching ratios for heavy neutrino decay patterns. In our numerical calculations below, we adopt the benchmark decay branching ratios of heavy neutrinos with $\Omega = I$ for NH and IH as shown in Table I. One can also obtain the decay branching fractions of charged leptons E_i^\pm as the relations in Eq. (8) apply.

III. PAIR PRODUCTION OF HEAVY LEPTONS AT MUON COLLIDER

The pair production channels of heavy triplet leptons at muon colliders include

- $\mu^+ \mu^- \rightarrow \gamma^*/Z^* \rightarrow E^+ E^-$,
- $W^+ W^- \rightarrow \gamma^*/Z^* \rightarrow E^+ E^-$, $\gamma/Z + \gamma/Z \rightarrow E^+ E^-$, $W^+ W^- \rightarrow NN, E^+ E^-$,
- $W^\pm + \gamma/Z \rightarrow W^{\pm*} \rightarrow E^\pm N$, $W^\pm + \gamma/Z \rightarrow E^\pm N$.

The Feynman diagrams of heavy triplet lepton pair productions in Type III Seesaw are collected in Fig. 1. They are given by the pure EW gauge interactions in Eq. (6) and not suppressed by the mixing $V_{\ell N}$. For c.m. energies $\sqrt{s} \gg M_W$, the initial muon beams substantially radiate EW gauge bosons under an approximately unbroken SM gauge symmetry. The vector bosons are treated as initial state partons and produce “inclusive” processes. We use MadGraph5_aMC@NLO [59] to calculate the VBF cross sections, by utilizing the leading-order framework of electroweak parton

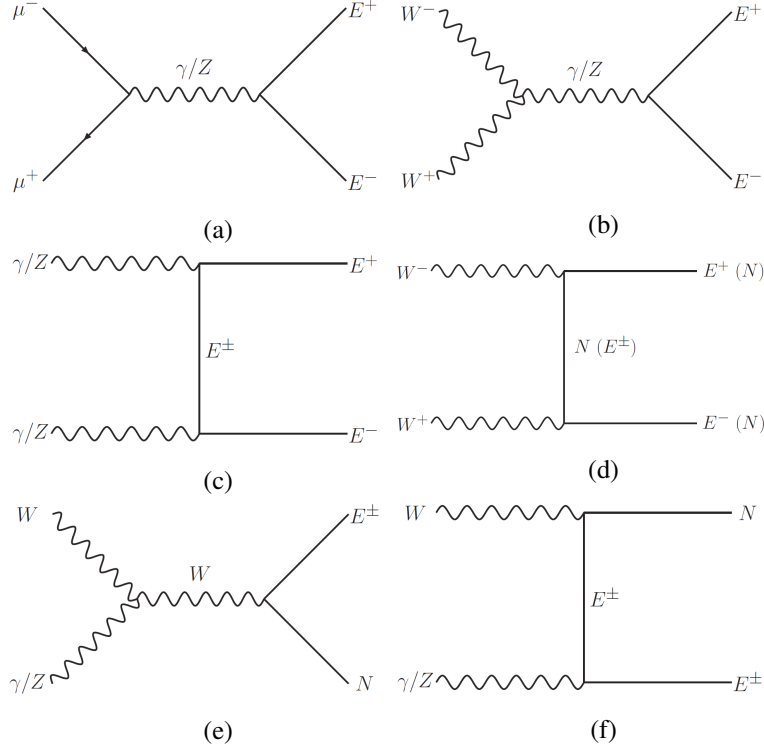


FIG. 1. Feynman diagrams of heavy triplet lepton pair productions in Type III Seesaw, including $\mu^+\mu^-$ annihilation (a) and VBF processes (b-f).

distribution functions (EW PDFs) [60–62] with a dynamical scale $Q = \sqrt{\hat{s}}/2$, where $\sqrt{\hat{s}}$ is the partonic c.m. energy. For the initial gauge bosons V_a and V_b , the VBF production cross section can be factorized as the product of the parton luminosity $d\mathcal{L}_{ab}/d\tau$ and the partonic cross section $\hat{\sigma}$ [60]

$$\sigma(\mu^+\mu^- \rightarrow F + X) = \int_{\tau_0}^1 d\tau \sum_{ab} \frac{d\mathcal{L}_{ab}}{d\tau} \hat{\sigma}(V_a V_b \rightarrow F),$$

$$\frac{d\mathcal{L}_{ab}}{d\tau} = \frac{1}{1 + \delta_{ab}} \int_{\tau}^1 \frac{d\xi}{\xi} \left[f_a(\xi, Q^2) f_b\left(\frac{\tau}{\xi}, Q^2\right) + (a \leftrightarrow b) \right], \quad (14)$$

where $F(X)$ denotes an exclusive final state (the underlying remnants), $f_a(\xi, Q^2)$ is the EW PDF for vector V_a with Q being the factorization scale, $\tau_0 = m_F^2/s$ and $\tau = \hat{s}/s$. By summing over all gauge boson initial states in Fig. 1, one can obtain the total cross section of the “inclusive” VBF production processes.

We consider three benchmark choices of muon collider energies and the corresponding integrated luminosities for illustration

$$\sqrt{s} = 3, 10 \text{ and } 30 \text{ TeV}, \quad \mathcal{L} = 1, 10 \text{ and } 90 \text{ ab}^{-1}. \quad (15)$$

The heavy triplet leptons are followed by the decays into charged leptons or active neutrinos as well as EW gauge bosons. We smeared the parton level events with an energy resolution of $\Delta E/E =$

2%. Note that we consider the hadronic decay of EW gauge bosons into two jets. The two jets generally form a fat jet here as the gauge bosons are from heavy triplet decay and thus are highly boosted. We perform the parton showering and detector simulation to identify the fat jets and then reconstruct the vector bosons efficiently. The hadronic decay branching fractions and the efficiencies of the gauge boson reconstruction are included in our numerical analysis. The details of this reconstruction will be described below. We also take a conservative way to estimate the significance as

$$\mathcal{S} = \frac{N_S}{\sqrt{N_S + N_B}} , \quad (16)$$

where N_S and N_B denote the signal and SM background event numbers, respectively.

A. E^+E^- Pair Production

We first perform the calculation of the pair production of heavy charged leptons. The E^+E^- productions are decomposed to $\mu^+\mu^-$ direct annihilation and the electroweak VBF processes initiated by γ/Z or W^+W^- . In Fig. 2, we show the production cross sections of E^+E^- as a function of \sqrt{s} (left) and M_E (right). The productions via $\mu^+\mu^-$ annihilation, VBF and their sum are represented as dashed lines, dotted lines and solid lines, respectively. The $\mu\mu$ annihilation cross sections approach $\sigma^{\text{Ann}} \sim \beta/s$ with the velocity as $\beta = \sqrt{1 - \frac{4M_E^2}{s}}$. Thus, they decrease with the increasing c.m. energy. Well above the threshold, the triplet mass can be ignored at high energies and the heavy charged leptons tend to be indistinguishable in this channel. On the other hand, the VBF cross sections σ^{VBF} are enhanced by collinear logarithm $\ln(\hat{s}/m_\mu^2)$ for photon or $\ln(\hat{s}/m_V^2)$ for massive gauge boson V at high beam energies. They are also very sensitive to the heavy lepton masses and decrease quickly with increasing M_E . The VBF process is thus important at low M_E and high c.m. energies.

We consider the above productions followed by two decay modes of E^\pm

$$E^\pm \rightarrow \nu W^\pm , \quad E^\pm \rightarrow \ell^\pm Z . \quad (17)$$

For the first mode, the SM neutrinos are summed over and thus one has $\text{BR}(E^\pm \rightarrow \sum_\nu \nu W^\pm) \approx 50\%$ according to the relation in Eq. (8). In the second mode, we only study the decay $E^\pm \rightarrow \mu^\pm Z$ for illustration and the decay branching fractions of the heavy neutrino in Table I apply here as $\text{BR}(N_i \rightarrow \ell^\pm W^\mp) \approx \text{BR}(E_i^\pm \rightarrow \ell^\pm Z)$ for degenerate triplet leptons. Note that we take the channel $E \rightarrow \mu Z$ here for illustrative estimation of the heavy triplet search prospect. The channel $E \rightarrow e Z$ can also be analyzed following the same strategies and their SM background analysis is even simpler as the electrons cannot come from the fermion line of initial states.

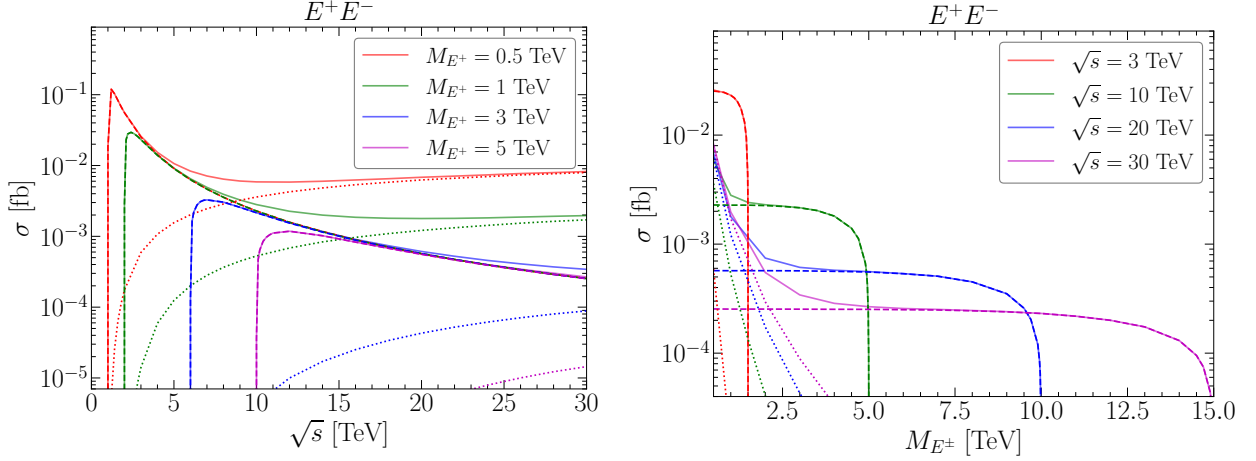


FIG. 2. Cross sections of E^+E^- pair production as a function of \sqrt{s} (left) and M_E (right) at muon colliders by $\mu^+\mu^-$ annihilation (dashed lines), VBF (dotted lines), and the sum (solid lines).

I. $E^+E^- \rightarrow W^+W^-\nu\bar{\nu}$

In this case, our signal is composed of W^+W^- and large missing energy induced by SM neutrinos. The SM background in this channel thus becomes

$$W^+W^-Z, \quad (18)$$

followed by decay $Z \rightarrow \nu\bar{\nu}$ and is generated by MadGraph at the parton level. We also consider both the $\mu^+\mu^-$ annihilation and VBF productions for the above background. In the beginning, the size of SM background is comparable to our signal. We thus employ the following judicious cuts to reduce the background:

- We take into account the W bosons identified in central region and set the rapidity cut as follows

$$|\eta(W)| < 3.0. \quad (19)$$

- For a few TeV E^\pm , the decay products from heavy triplet lepton are very energetic as shown in Fig. 3 (left) ¹. We therefore tight up the kinematical cut with

$$p_T^{\max}(W) > \frac{M_E}{2}, \quad (20)$$

for the leading W boson.

¹ The differential cross sections of the $\mu\mu$ annihilation and VBF processes are individually weighted by their total cross sections and summed together here.

- To remove the W^+W^-Z background with neutrinos from Z boson decay as seen in the right panel of Fig. 3, we require the events with large missing energy from neutrinos

$$\cancel{E}_T > \frac{M_E}{4} . \quad (21)$$

As a result, the SM background can be significantly suppressed.

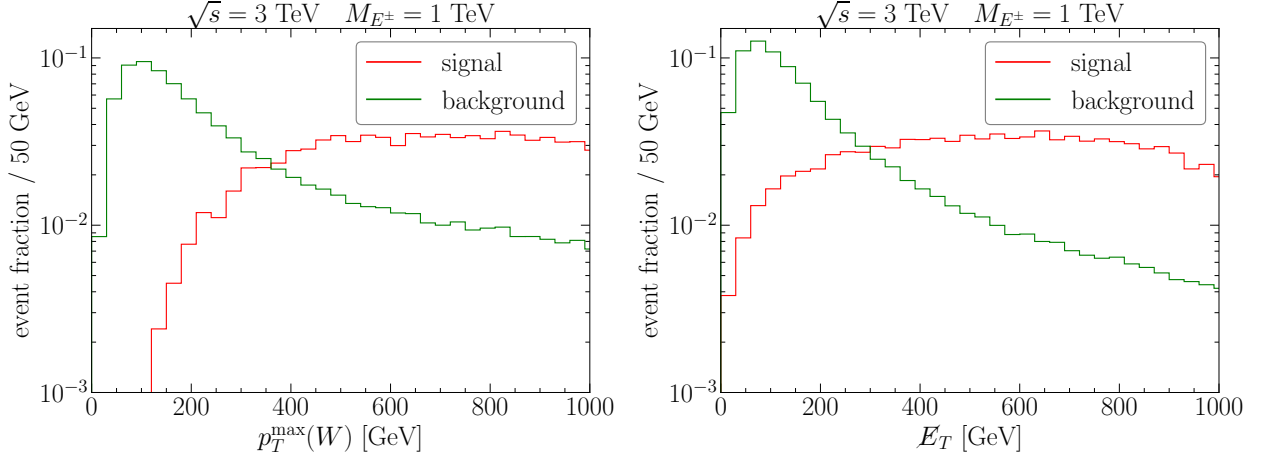


FIG. 3. The normalized $p_T^{\max}(W)$ (left) and \cancel{E}_T (right) distributions of the signal $E^+E^- \rightarrow W^+W^-\nu\bar{\nu}$ and the SM background for $\sqrt{s} = 3$ TeV and $M_E = 1$ TeV.

We then perform the local significance analysis. The event numbers of signal (N_S) and background (N_B) are given by

$$\begin{aligned} N_S &= (\sigma_S^{\text{Ann}} \epsilon_S^{\text{Ann}} \epsilon_{S,W}^{\text{Ann}} + \sigma_S^{\text{VBF}} \epsilon_S^{\text{VBF}} \epsilon_{S,W}^{\text{VBF}}) \times \text{BR}(E^\pm \rightarrow W^\pm \nu)^2 \times \mathcal{L} \times \text{BR}(W^\pm \rightarrow q\bar{q}')^2 , \\ N_B &= (\sigma_B^{\text{Ann}} \epsilon_B^{\text{Ann}} \epsilon_{B,W}^{\text{Ann}} + \sigma_B^{\text{VBF}} \epsilon_B^{\text{VBF}} \epsilon_{B,W}^{\text{VBF}}) \times \text{BR}(Z \rightarrow \nu\bar{\nu}) \times \mathcal{L} \times \text{BR}(W^\pm \rightarrow q\bar{q}')^2 , \end{aligned} \quad (22)$$

where σ_S is the signal cross section, σ_B is the cross section of the SM background W^+W^-Z , the superscripts “Ann” and “VBF” denote $\mu^+\mu^-$ direct annihilation and VBF process, respectively, $\epsilon_{S,B}$ represent the efficiencies of the above cuts and \mathcal{L} denotes the integrated luminosity. In practice, the W bosons subsequently decay into leptonic or hadronic products. Here and below we consider the hadronic decay of vector bosons into a dijet. As being from heavy lepton decay, the vector bosons are highly boosted and the two jets are likely to merge into a single fat jet J . To perform the simulation of vector boson reconstruction, we pass the parton-level events to Pythia 8 [63] and Delphes 3 [64] for parton shower and detector simulation, respectively. We choose the detector card of muon collider in the latest version of Delphes for detector-level simulation. The jets from W decay are clustered in FastJet [65] and we require at least two fat jets. The fat jet is reconstructed via the “Valencia” algorithm with $R = 0.5$ and the one with $65 < M_J < 95$ GeV ($75 < M_J < 105$ GeV for Z boson used in Sec. III B) is identified as boosted W candidate. $\epsilon_{S,W}$ and $\epsilon_{B,W}$ in Eq. (22) are the efficiencies of the vector boson reconstruction.

In Fig. 4, we show the integrated luminosities required for 3σ and 5σ significance at muon collider with $\sqrt{s} = 3$ TeV (left) and $\sqrt{s} = 10$ TeV (right). One can see that the charged triplet lepton as heavy as one-half of the colliding energy can be probed. A 5σ significance can be reached through the $E^+E^- \rightarrow W^+W^-\nu\bar{\nu}$ process with the integrated luminosity below 0.1 ab^{-1} for $\sqrt{s} = 3$ TeV and 2 ab^{-1} for $\sqrt{s} = 10$ TeV. Despite this optimistic result, however, we are not able to reconstruct the heavy leptons due to the missing neutrinos from E^\pm decay. Moreover, the different neutrino mass patterns and the three triplet leptons cannot be identified and distinguished through this process as the missing neutrinos lose lepton flavor information in detector. We need to discuss other signal channels in the following section to reveal the neutrino characteristics.

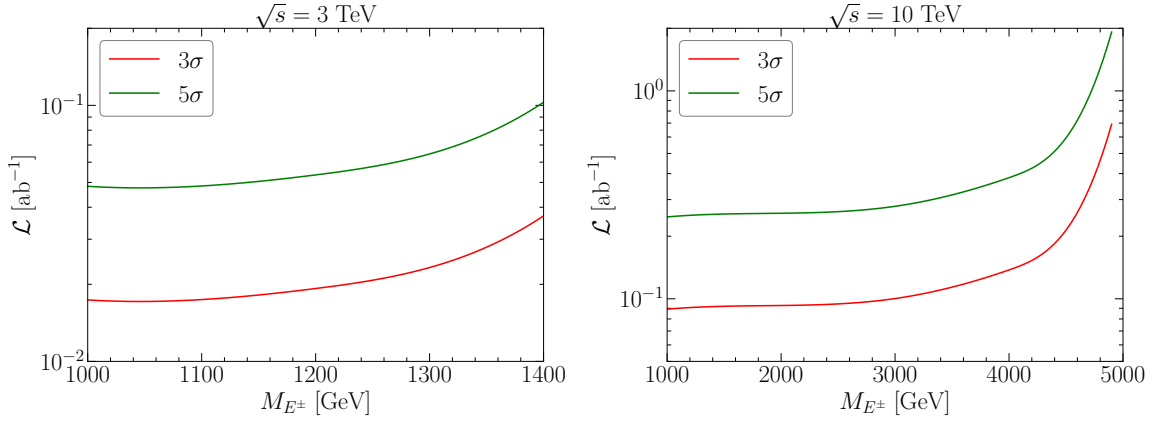


FIG. 4. The integrated luminosities for 3σ and 5σ significance versus M_E for $E^+E^- \rightarrow W^+W^-\nu\bar{\nu}$ in muon collider with $\sqrt{s} = 3$ TeV (left) and 10 TeV (right).

2. $E^+E^- \rightarrow ZZ\mu^+\mu^-$

Next, we discuss the E^+E^- pair production followed by $E^\pm \rightarrow \ell^\pm Z$ decay mode. In this case, we only consider the decay channel $E^\pm \rightarrow \mu^\pm Z$ for illustration. The signal is thus composed of two Z bosons and $\mu^+\mu^-$. The SM background is also categorized into $\mu^+\mu^-$ annihilation and VBF production. Since there are two muons in the final states of this channel, we employ the following basic cuts

$$p_T(\mu) > 50 \text{ GeV}, \quad |\eta(\mu, Z)| < 3.0. \quad (23)$$

We also employ the judicious cuts to reduce the background:

- For the energetic products from a few TeV E^\pm , we set the following kinematical cuts

$$p_T^{\max}(Z) > \frac{M_E}{3}, \quad p_T^{\max}(\mu) > \frac{M_E}{3}. \quad (24)$$

- Since the final particles μ^\pm and Z are both observable in detector, one can reconstruct the triplet lepton E^\pm . To reconstruct heavy fermion E^\pm , we pair the final particles (Z, μ) by taking advantage of the feature that they have equal masses $M_{Z_1\mu_1} = M_{Z_2\mu_2}$, which is in order to make sure they come from the correct mother particle. Then we take the invariant masses close to M_E with

$$|M_{Z\mu} - M_E| < \frac{M_E}{5} . \quad (25)$$

The reconstructed masses are shown in Fig. 5.

These cuts help to reduce the SM backgrounds.

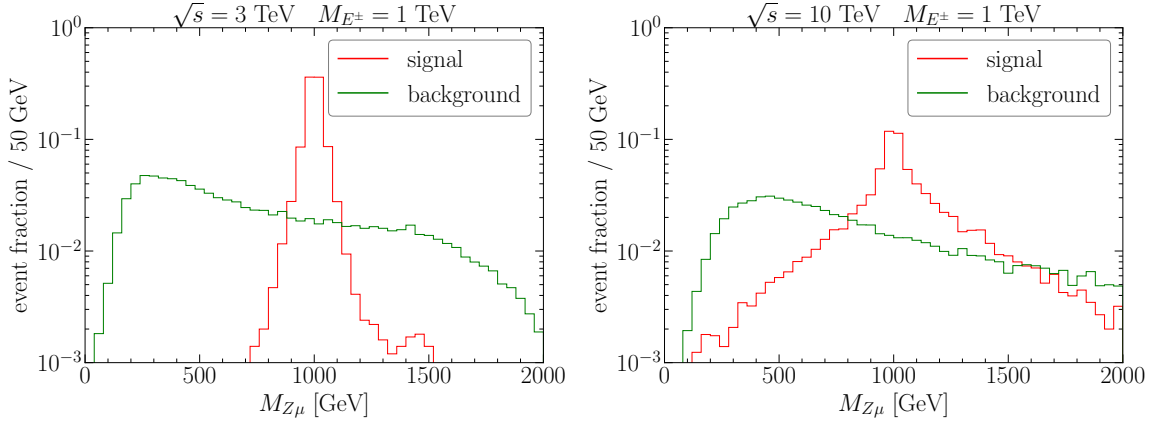


FIG. 5. The invariant mass $M_{Z\mu}$ distribution of the signal $E^+E^- \rightarrow ZZ\mu^+\mu^-$ and the background for $M_E = 1$ TeV, $\sqrt{s} = 3$ TeV (left) and 10 TeV (right).

For the local significance analysis, we apply the benchmark decay branching fraction of $E^\pm \rightarrow \mu^\pm Z$ for $N_{1,2,3}$ in both NH and IH mass patterns in Table I. As a result, in Fig. 6, we show the integrated luminosities for 5σ significance in the muon collider with $\sqrt{s} = 3$ TeV (left) and $\sqrt{s} = 10$ TeV (right). With the optimistic integrated luminosity of 1 ab^{-1} for $\sqrt{s} = 3$ TeV or 10 ab^{-1} for $\sqrt{s} = 10$ TeV, both N_2 and N_3 can be discovered. One can distinguish E_2 and E_3 for IH and they are not distinguishable for NH. To discover N_1 , we need much higher luminosity. A 5σ significance for $\sqrt{s} = 3$ TeV will be reached with the integrated luminosity above 1 ab^{-1} for NH and IH. The reachable branching ratio of $E^\pm \rightarrow Z\mu^\pm$ corresponding to 3σ and 5σ significance is given in Fig. 7, with $\sqrt{s} = 3$ TeV, $\mathcal{L} = 1 \text{ ab}^{-1}$ (left) and $\sqrt{s} = 10$ TeV, $\mathcal{L} = 10 \text{ ab}^{-1}$ (right). One can see that $\text{BR}(E^\pm \rightarrow Z\mu^\pm)$ below 10.7% (6.4%) can be reached for 5σ (3σ) significance for $\sqrt{s} = 3$ TeV and $\mathcal{L} = 1 \text{ ab}^{-1}$. For $\sqrt{s} = 10$ TeV and $\mathcal{L} = 10 \text{ ab}^{-1}$, the branching fraction can be as large as 13.0% (7.8%) for 5σ (3σ) significance.

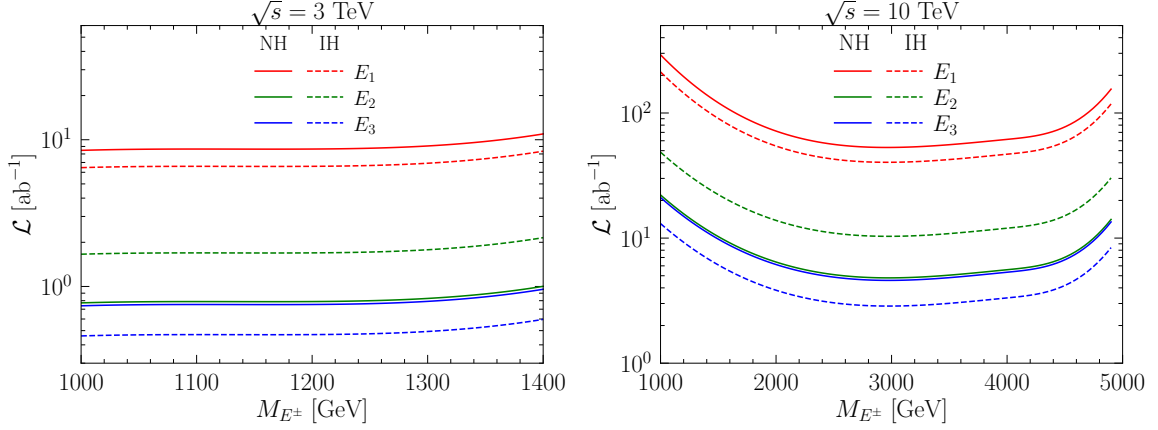


FIG. 6. The integrated luminosities for 5σ significance versus M_E for $E^+E^- \rightarrow ZZ\mu^+\mu^-$ in muon colliders with $\sqrt{s} = 3$ TeV (left) and 10 TeV (right), for $E_{1,2,3}$ and NH (solid lines) or IH (dashed lines).

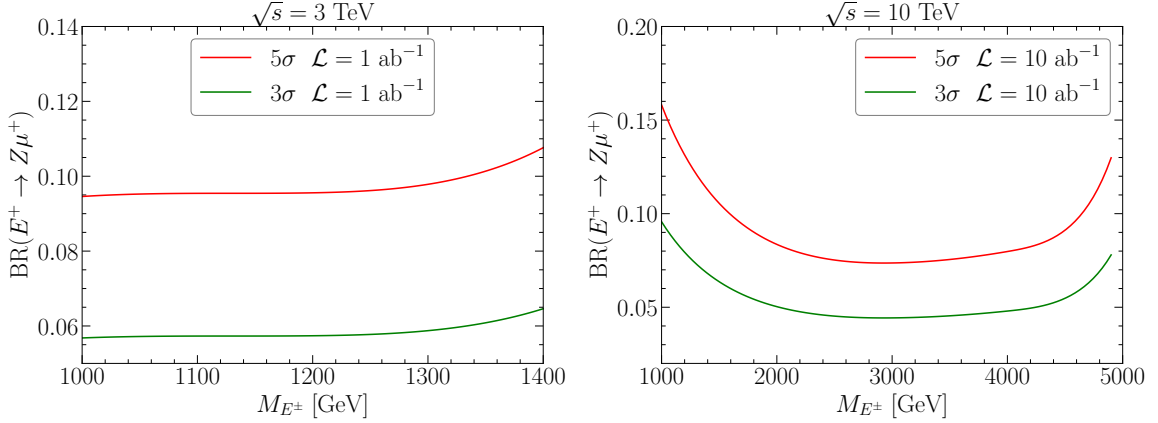


FIG. 7. The reachable branching ratio of $E^\pm \rightarrow Z\mu^\pm$ corresponding to 3σ and 5σ significance versus M_E for $E^+E^- \rightarrow ZZ\mu^+\mu^-$ in muon colliders with $\sqrt{s} = 3$ TeV, $\mathcal{L} = 1 \text{ ab}^{-1}$ (left) and $\sqrt{s} = 10$ TeV, $\mathcal{L} = 10 \text{ ab}^{-1}$ (right).

B. $E^\pm N$ Associated Production

The $E^\pm N$ associated production is only from VBF processes initiated by γ/Z and W^\pm . The cross sections are shown in Fig. 8, as a function of \sqrt{s} (left) and $M_{E(N)}$ (right), and are enhanced by EW PDF at higher beam energies. We find that muon collider with energy 3 TeV or 10 TeV can not generate enough signal events, and we thus take $\sqrt{s} = 30$ TeV in the following studies. For $\sqrt{s} = 30$ TeV, under the assumption that the masses of charged and neutral triplet leptons are degenerate, the cross sections are less than 10^{-3} fb for triplet lepton masses greater than 1 TeV. The associated production of charged and neutral heavy leptons followed by decay modes $E^\pm \rightarrow \ell^\pm Z$ and $N \rightarrow \ell^\pm W^\mp$ can lead to the rare signature of lepton number violation with same-sign charged

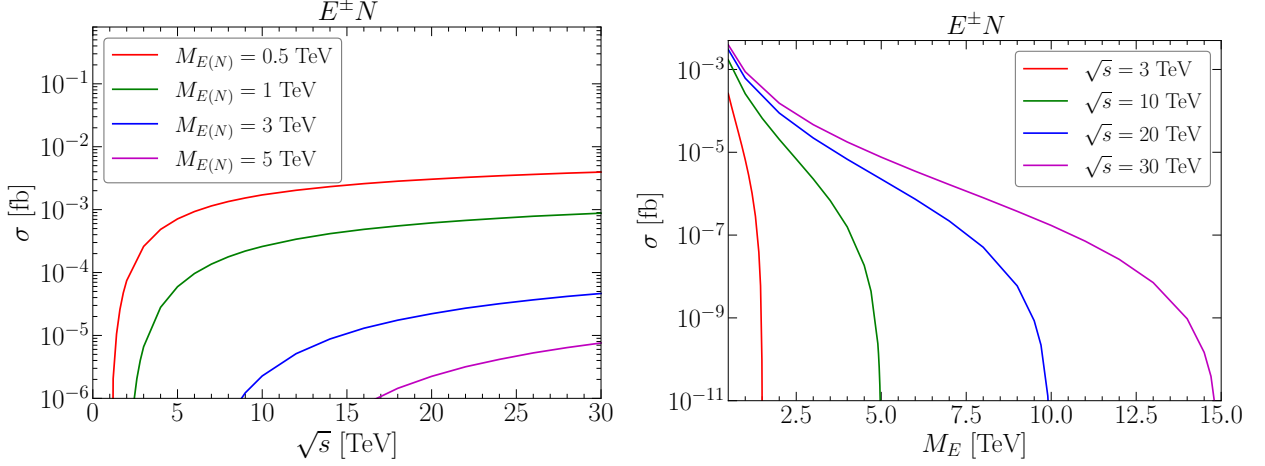


FIG. 8. Cross sections of $E^\pm N$ associated production as a function of \sqrt{s} (left) and $M_{E,N}$ (right) at muon colliders by VBF process.

leptons

$$E^\pm N \rightarrow ZW^\mp \mu^\pm \mu^\pm. \quad (26)$$

We will only consider the sensitivity of muon collider with $\sqrt{s} = 30$ TeV to the distinctive LNV signature.

The leading SM background to this channel becomes

$$ZW^\mp W^\pm W^\pm, \quad (27)$$

followed by decay $W^\pm \rightarrow \mu^\pm \nu_\mu (\bar{\nu}_\mu)$. We simulate VBF production of the above background using MadGraph at the parton level. Firstly, we employ the basic cuts for the gauge bosons in final states

$$p_T(W, Z) > 300 \text{ GeV}, \quad |\eta(W, Z)| < 3.0. \quad (28)$$

We also employ further judicious cuts to reduce the background

- For a few TeV E^\pm and N , we set the advanced p_T cuts on the gauge bosons as follows

$$p_T(W) > \frac{M_N}{3}, \quad p_T(Z) > \frac{M_E}{3}. \quad (29)$$

- Note that the ν_μ or $\bar{\nu}_\mu$ from W boson decay only appear in the SM background. For our signal, the $E^\pm N$ or NN production is induced by the VBF process in which there is no missing neutrino. Nevertheless, in the process of event analysis, we consider the smearing of the transverse momentum with a resolution of the detector mentioned below Eq. (15). As a result, there appears a small transverse missing energy in the signal. As shown in left panel of Fig. 9, we veto the events with large missing energy from neutrinos

$$\cancel{E}_T < 500 \text{ GeV}. \quad (30)$$

- To suppress the continuum background, we reconstruct the heavy lepton E^\pm and N . Firstly, we pair the final particles W_μ and Z_μ according to the feature that the real combination comes from heavy triplets with degenerate masses. The reconstructed heavy lepton masses are shown in the right panel of Fig. 9. Then we take the mass windows of the resonances

$$|M_{Z\mu_1} - M_E| < \frac{M_E}{5}, \quad |M_{W\mu_2} - M_N| < \frac{M_N}{5}. \quad (31)$$

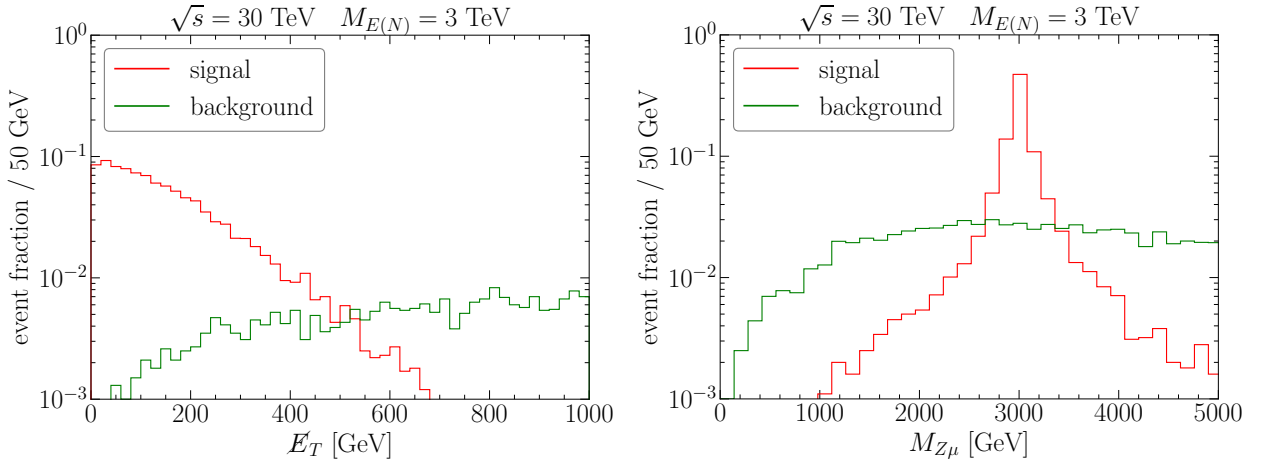


FIG. 9. The normalized \cancel{E}_T (left) and invariant mass $M_{Z\mu}$ (right) distributions of the heavy leptons in the signal $E^\pm N \rightarrow ZW^\mp \mu^\pm \mu^\pm$ and the background for $\sqrt{s} = 30$ TeV and $M_{E(N)} = 3$ TeV.

One can efficiently suppress the SM background and the cut efficiency becomes $\epsilon_B \sim 0.1\%$ by using the above cuts, so it is enough to only consider the signal events. The event number of signal is given by

$$N_S = \sigma_S^{\text{VBF}} \times \epsilon_S^{\text{VBF}} \times \epsilon_{S,W/Z}^{\text{VBF}} \times \text{BR}(E^\pm \rightarrow Z\mu^\pm) \times \text{BR}(N \rightarrow W^\mp \mu^\pm) \times \mathcal{L} \times \text{BR}(W^\pm \rightarrow q\bar{q}') \times \text{BR}(Z \rightarrow q\bar{q}), \quad (32)$$

where $\epsilon_{S,W/Z}^{\text{VBF}}$ denotes the efficiency of reconstructing W and Z bosons, $\text{BR}(E^\pm \rightarrow Z\mu^\pm) \approx \text{BR}(N \rightarrow W^\mp \mu^\pm)$ as shown in Table I. The number of signal events at muon collider with $\sqrt{s} = 30$ TeV is shown in left panel of Fig. 10, with the integrated luminosity of 90 ab^{-1} . One can see that the three heavy triplet leptons and two neutrino mass patterns exhibit different event numbers. For $M_{E(N)}$ greater than 6 TeV, it is impossible to receive more than one signal event. The reachable branching ratio of $E^\pm \rightarrow Z\mu^\pm$ and $N \rightarrow W^\mp \mu^\pm$ corresponding to $N_S = 5$ and $N_S = 10$ is given in the right panel of Fig. 10. $\text{BR}(E^\pm \rightarrow Z\mu^\pm)$ below 40.3% (28.5%) can be reached for $N_S = 10$ ($N_S = 5$) and $M_{E(N)} < 5$ TeV at muon collider with $\sqrt{s} = 30$ TeV and $\mathcal{L} = 90 \text{ ab}^{-1}$.

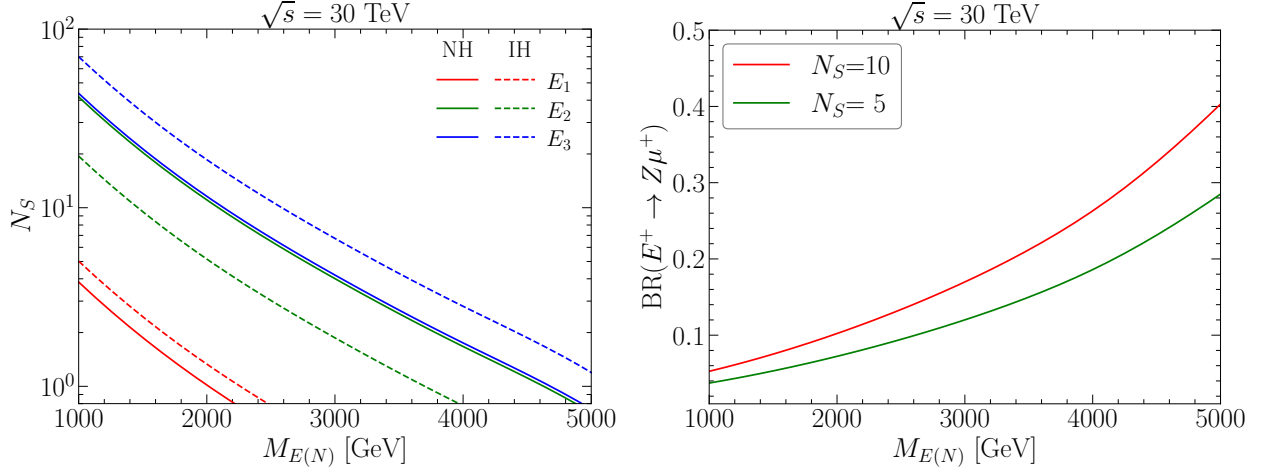


FIG. 10. Left: The number of signal events versus $M_{E(N)}$ for $E^\pm N \rightarrow W^\mp Z\mu^\pm\mu^\pm$ at muon collider with $\sqrt{s} = 30$ TeV and $\mathcal{L} = 90 \text{ ab}^{-1}$, for $E(N)_{1,2,3}$ and NH (solid lines) or IH (dashed lines). Right: The reachable branching ratio of $E^\pm \rightarrow Z\mu^\pm$ or $N \rightarrow W^\mp\mu^\pm$ corresponding to $N_S = 5$ and $N_S = 10$ versus $M_{E(N)}$ for $E^\pm N \rightarrow W^\mp Z\mu^\pm\mu^\pm$ at muon collider with $\sqrt{s} = 30$ TeV and $\mathcal{L} = 90 \text{ ab}^{-1}$.

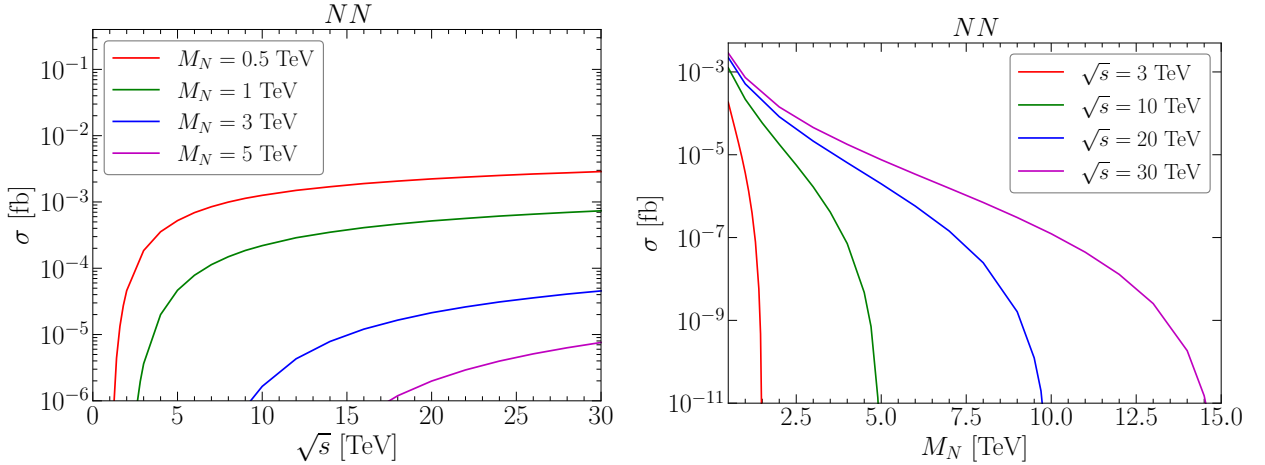


FIG. 11. Cross sections of NN pair production as a function of \sqrt{s} (left) and M_N (right) at muon colliders by VBF process.

C. NN Pair Production

In this subsection, we discuss the NN pair production from VBF process initiated by W^+W^- . The VBF cross sections as a function of \sqrt{s} and M_N are shown in Fig. 11. The cross sections are slightly smaller than those of $E^\pm N$ associated production as there is only W^+W^- initiated VBF process. We will only consider the distinctive LNV signature at muon collider with $\sqrt{s} = 30$ TeV, i.e.,

$$NN \rightarrow W^\mp W^\mp \mu^\pm \mu^\pm. \quad (33)$$

The leading SM background becomes

$$W^+W^+W^-W^-, \quad (34)$$

followed by decay $W^\pm \rightarrow \mu^\pm \nu_\mu (\bar{\nu}_\mu)$ for one pair of same-sign W bosons. The judicious cuts to reduce the background are

- For a few TeV N , we set the advanced p_T cuts for the leading W boson and μ^\pm as follows

$$p_T^{\max}(W) > \frac{M_N}{3}, \quad p_T^{\max}(\mu) > \frac{M_N}{3}. \quad (35)$$

- Since the ν_μ or $\bar{\nu}_\mu$ only appears in the SM background, we can set the cuts on missing energy from neutrinos as shown in left panel of Fig. 12

$$\cancel{E}_T < 500 \text{ GeV}. \quad (36)$$

- In order to reconstruct the heavy neutrino N , we pair the particles $W\mu$ according to the feature that the real combination comes from heavy triplets with degenerate masses. The invariant mass distribution is shown in the right panel of Fig. 12. Then we take the mass windows of the resonances

$$|M_{W\mu} - M_N| < \frac{M_N}{5}. \quad (37)$$

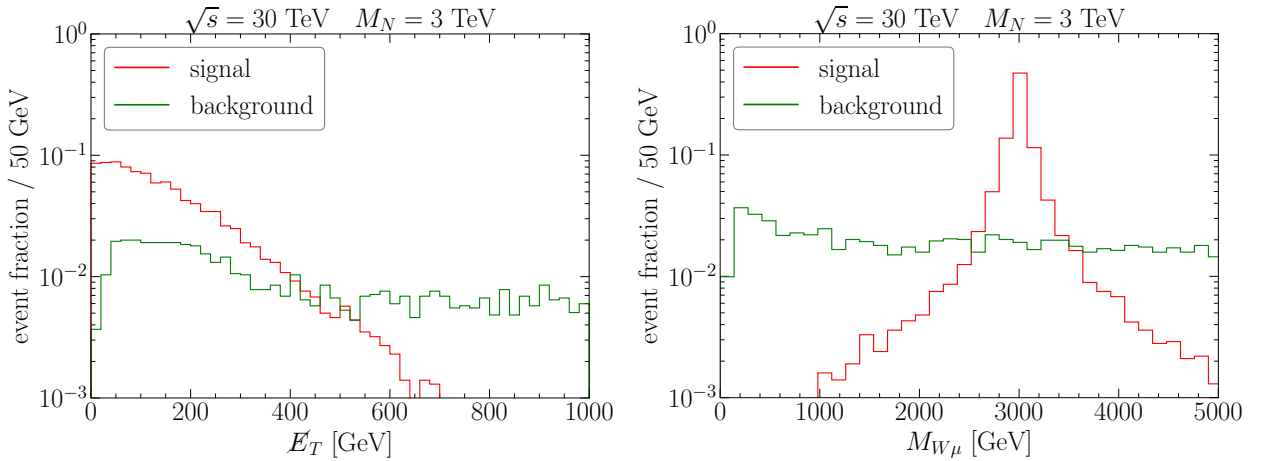


FIG. 12. The normalized \cancel{E}_T (left) and invariant mass $M_{W\mu}$ (right) distributions of the heavy leptons in the signal $NN \rightarrow W^\mp W^\mp \mu^\pm \mu^\pm$ and the background for $\sqrt{s} = 30 \text{ TeV}$ and $M_N = 3 \text{ TeV}$.

Since the SM background is extremely suppressed, we will only consider the signal events. The event number of signal is given by

$$N_S = \sigma_S^{\text{VBF}} \times \epsilon_S^{\text{VBF}} \times \epsilon_{S,W}^{\text{VBF}} \times \text{BR}^2(N \rightarrow W^\mp \mu^\pm) \times \mathcal{L} \times \text{BR}(W^\pm \rightarrow q\bar{q}')^2 \times 2, \quad (38)$$

where the factor 2 accounts for the charge conjugation of decay products, as shown in the left panel of Fig. 13. For $M_N \gtrsim 6$ TeV, it is almost impossible to obtain more than one signal event. The reachable branching ratio of $N \rightarrow W^\mp \mu^\pm$ is given in the right panel of Fig. 13. $\text{BR}(N \rightarrow W^\mp \mu^\pm)$ below 22.2% (15.8%) can be reached for $N_S = 10$ ($N_S = 5$) and $M_N < 5$ TeV at muon collider with $\sqrt{s} = 30$ TeV and $\mathcal{L} = 90 \text{ ab}^{-1}$.

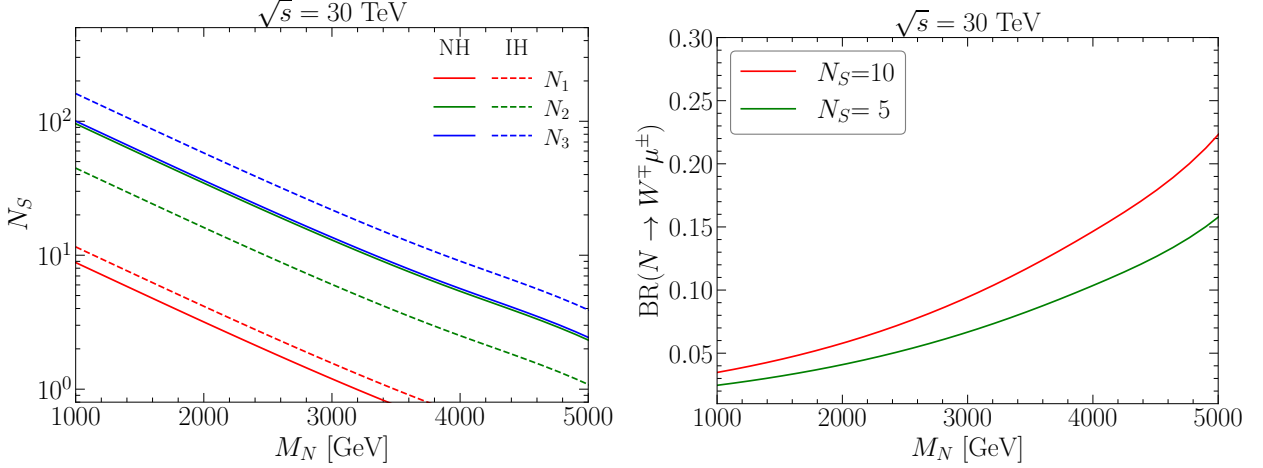


FIG. 13. Left: The number of signal events versus M_N for $NN \rightarrow W^\mp W^\mp \mu^\pm \mu^\pm$ at muon collider with $\sqrt{s} = 30$ TeV and $\mathcal{L} = 90 \text{ ab}^{-1}$, for $N_{1,2,3}$ and NH (solid lines) or IH (dashed lines). Right: The reachable branching ratio of $N \rightarrow W^\mp \mu^\pm$ corresponding to $N_S = 5$ and $N_S = 10$ versus M_N for $NN \rightarrow W^\mp W^\mp \mu^\pm \mu^\pm$ at muon collider with $\sqrt{s} = 30$ TeV and $\mathcal{L} = 90 \text{ ab}^{-1}$.

Finally, we comment on the decay length and possible displaced vertex of heavy triplet leptons. The total decay widths of heavy triplet leptons are proportional to $|V_{\ell N}|^2 \sim m_\nu/M_\Sigma$ which may lead to long decay length. We calculate the decay length of the triplet leptons by the formula $L = \gamma\beta c\tau$, where $\tau = 1/\Gamma$ is the life-time, γ is the boost factor and β is the ratio of velocity v_Σ to the speed of light c . The product $\gamma\beta$ can then be given by $\gamma\beta = \sqrt{E_\Sigma^2/M_\Sigma^2 - 1}$. To evaluate the displaced vertex, we take into account the light neutrino masses with the minimal one being 10^{-4} eV. In our analysis, E_Σ is roughly taken to be $\sqrt{s}/2$ in the c.m. frame. Fig. 14 shows the decay length versus M_N for N_i ($i = 1, 2, 3$) and $\Omega = I$ at different collider energies. We find that in most cases the decay length is less than $\mathcal{O}(1)$ mm and the heavy leptons can be viewed as decaying promptly. Only for the cases of N_1 in NH and N_3 in IH, the typical decay length can be longer than 1 mm in relatively low mass region. In particular, for $M_N \sim 1$ TeV and $\sqrt{s} = 30$ TeV, the decay length could be as large as 20 mm, which is sufficiently long to perform the displaced vertex searches [31, 34]. If this clear difference is observed in future, it could serve as an indication to distinguish the heavy leptons and neutrino patterns.

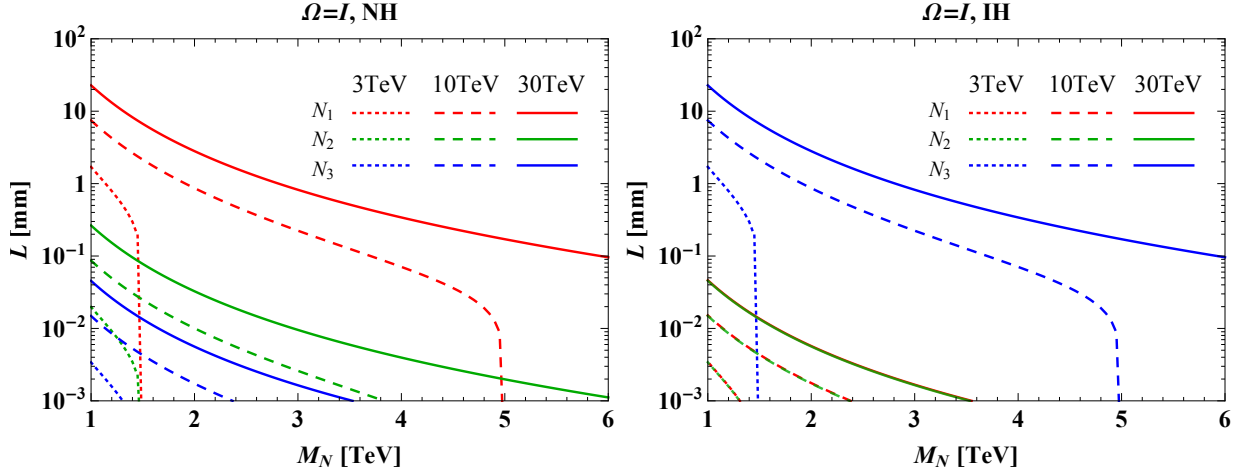


FIG. 14. Decay length versus M_N for different heavy neutrinos N_i ($i = 1, 2, 3$) and different neutrino mass hierarchies NH (left) and IH (right) at muon collider with energy 3 TeV (dotted line), 10 TeV (dashed line) and 30 TeV (solid line) respectively.

IV. CONCLUSION

We perform a study of search for heavy triplet leptons in Type III Seesaw mechanism at future high-energy and high-luminosity muon colliders. The impact of up-to-date neutrino oscillation results is taken into account on neutrino mass model and the consequent lepton flavor signatures of heavy leptons in Type III Seesaw. According to the asymptotic behavior, the heavy lepton branching fractions exhibit $\text{BR}(E^\pm \rightarrow \sum_\nu \bar{\nu} W^\pm) \approx 50\%$ and $\text{BR}(N \rightarrow \ell^\pm W^\mp) \approx \text{BR}(E^\pm \rightarrow \ell^\pm Z)$ for $M_{E(N)} \gg M_W$. The three heavy leptons in the Casas-Ibarra parametrization with diagonal unity matrix can be distinguished in terms of their decay modes.

We consider the pair production of charged triplet leptons $E^+ E^-$ through both $\mu^+ \mu^-$ annihilation and VBF processes. The charged triplet lepton as heavy as one-half of colliding energy can be probed. A 5σ significance can be reached through the $E^+ E^- \rightarrow W^+ W^- \nu \bar{\nu}$ process with the integrated luminosity below 0.1 ab^{-1} for $\sqrt{s} = 3 \text{ TeV}$ and 2 ab^{-1} for $\sqrt{s} = 10 \text{ TeV}$. The $E^+ E^- \rightarrow ZZ \ell^+ \ell^-$ channel can be further utilized to fully reconstruct the three triplet leptons and distinguish neutrino mass patterns. $\text{BR}(E^\pm \rightarrow Z \mu^\pm)$ below 10.7% (6.4%) can be reached for 5σ (3σ) significance for $\sqrt{s} = 3 \text{ TeV}$ and $\mathcal{L} = 1 \text{ ab}^{-1}$.

The associated production $E^\pm N$ and the pair production of heavy neutrinos NN are only induced by VBF processes and lead to rare LNV signature. We study the search potential of LNV processes at future high-energy muon collider with $\sqrt{s} = 30 \text{ TeV}$. Through $E^\pm N$ (NN) production, $\text{BR}(N \rightarrow \mu^\pm W^\mp)$ below 40.3% (22.2%) can be reached for 10 signal events and $M_{E(N)} < 5 \text{ TeV}$ at muon collider with $\sqrt{s} = 30 \text{ TeV}$ and $\mathcal{L} = 90 \text{ ab}^{-1}$.

ACKNOWLEDGMENTS

We would like to thank Tao Han for very useful discussions. T.L. is supported by the National Natural Science Foundation of China (Grant No. 11975129, 12035008) and “the Fundamental Research Funds for the Central Universities”, Nankai University (Grants No. 63196013). C.Y.Y. is supported in part by the Grants No. NSFC-11975130, No. NSFC-12035008, No. NSFC-12047533, the Helmholtz-OCPC International Postdoctoral Exchange Fellowship Program, the National Key Research and Development Program of China under Grant No. 2017YFA0402200 and the China Postdoctoral Science Foundation under Grant No. 2018M641621.

-
- [1] S. Weinberg, *Phys. Rev. Lett.* **43**, 1566 (1979).
 - [2] E. Ma, *Phys. Rev. Lett.* **81**, 1171 (1998), [arXiv:hep-ph/9805219](#).
 - [3] P. Minkowski, *Phys. Lett. B* **67**, 421 (1977).
 - [4] T. Yanagida, *Conf. Proc. C* **7902131**, 95 (1979).
 - [5] M. Gell-Mann, P. Ramond, and R. Slansky, *Conf. Proc. C* **790927**, 315 (1979), [arXiv:1306.4669 \[hep-th\]](#).
 - [6] S. Glashow, *NATO Sci. Ser. B* **61**, 687 (1980).
 - [7] R. N. Mohapatra and G. Senjanovic, *Phys. Rev. Lett.* **44**, 912 (1980).
 - [8] R. E. Shrock, *Phys. Rev. D* **24**, 1232 (1981).
 - [9] J. Schechter and J. Valle, *Phys. Rev. D* **22**, 2227 (1980).
 - [10] W. Konetschny and W. Kummer, *Phys. Lett. B* **70**, 433 (1977).
 - [11] T. P. Cheng and L.-F. Li, *Phys. Rev. D* **22**, 2860 (1980).
 - [12] G. Lazarides, Q. Shafi, and C. Wetterich, *Nucl. Phys. B* **181**, 287 (1981).
 - [13] R. N. Mohapatra and G. Senjanovic, *Phys. Rev. D* **23**, 165 (1981).
 - [14] R. Foot, H. Lew, X. G. He, and G. C. Joshi, *Z. Phys. C* **44**, 441 (1989).
 - [15] J. Kersten and A. Y. Smirnov, *Phys. Rev. D* **76**, 073005 (2007), [arXiv:0705.3221 \[hep-ph\]](#).
 - [16] K. Moffat, S. Pascoli, and C. Weiland, (2017), [arXiv:1712.07611 \[hep-ph\]](#).
 - [17] Y. Abe *et al.* (Double Chooz), *Phys. Rev. Lett.* **108**, 131801 (2012), [arXiv:1112.6353 \[hep-ex\]](#).
 - [18] J. K. Ahn *et al.* (RENO), *Phys. Rev. Lett.* **108**, 191802 (2012), [arXiv:1204.0626 \[hep-ex\]](#).
 - [19] F. P. An *et al.* (Daya Bay), *Phys. Rev. Lett.* **108**, 171803 (2012), [arXiv:1203.1669 \[hep-ex\]](#).
 - [20] K. Abe *et al.* (T2K), *Phys. Rev. D* **103**, 112008 (2021), [arXiv:2101.03779 \[hep-ex\]](#).
 - [21] M. A. Acero *et al.* (NOvA), (2021), [arXiv:2108.08219 \[hep-ex\]](#).
 - [22] K. Abe *et al.* (Hyper-Kamiokande Proto-), *PTEP* **2015**, 053C02 (2015), [arXiv:1502.05199 \[hep-ex\]](#).
 - [23] Z. Djurcic *et al.* (JUNO), (2015), [arXiv:1508.07166 \[physics.ins-det\]](#).
 - [24] R. Acciarri *et al.* (DUNE), (2015), [arXiv:1512.06148 \[physics.ins-det\]](#).
 - [25] A. Arhrib, B. Bajc, D. K. Ghosh, T. Han, G.-Y. Huang, I. Puljak, and G. Senjanovic, *Phys. Rev. D* **82**, 053004 (2010), [arXiv:0904.2390 \[hep-ph\]](#).

- [26] T. Li and X.-G. He, *Phys. Rev. D* **80**, 093003 (2009), [arXiv:0907.4193 \[hep-ph\]](#).
- [27] C. Biggio and F. Bonnet, *Eur. Phys. J. C* **72**, 1899 (2012), [arXiv:1107.3463 \[hep-ph\]](#).
- [28] P. Bandyopadhyay, S. Choi, E. J. Chun, and K. Min, *Phys. Rev. D* **85**, 073013 (2012), [arXiv:1112.3080 \[hep-ph\]](#).
- [29] J. A. Aguilar-Saavedra, P. M. Boavida, and F. R. Joaquim, *Phys. Rev. D* **88**, 113008 (2013), [arXiv:1308.3226 \[hep-ph\]](#).
- [30] Y. Cai, T. Han, T. Li, and R. Ruiz, *Front. in Phys.* **6**, 40 (2018), [arXiv:1711.02180 \[hep-ph\]](#).
- [31] S. Jana, N. Okada, and D. Raut, (2020), [arXiv:1911.09037 \[hep-ph\]](#).
- [32] A. Das and S. Mandal, *Nucl. Phys. B* **966**, 115374 (2021), [arXiv:2006.04123 \[hep-ph\]](#).
- [33] S. Ashanujjaman and K. Ghosh, *Phys. Lett. B* **819**, 136403 (2021), [arXiv:2102.09536 \[hep-ph\]](#).
- [34] C. Sen, P. Bandyopadhyay, S. Dutta, and A. KT, *Eur. Phys. J. C* **82**, 230 (2022), [arXiv:2107.12442 \[hep-ph\]](#).
- [35] S. Ashanujjaman and K. Ghosh, *Phys. Lett. B* **825**, 136889 (2022), [arXiv:2111.07949 \[hep-ph\]](#).
- [36] D. Goswami and P. Poullose, *Eur. Phys. J. C* **78**, 42 (2018), [arXiv:1702.07215 \[hep-ph\]](#).
- [37] A. Das, S. Mandal, and T. Modak, *Phys. Rev. D* **102**, 033001 (2020), [arXiv:2005.02267 \[hep-ph\]](#).
- [38] P. Bandyopadhyay, A. Karan, and C. Sen, (2020), [arXiv:2011.04191 \[hep-ph\]](#).
- [39] S. Bhattacharya, S. Jahedi, and J. Wudka, *JHEP* **05**, 009 (2022), [arXiv:2106.02846 \[hep-ph\]](#).
- [40] A. M. Sirunyan et al. (CMS), *Phys. Rev. Lett.* **119**, 221802 (2017), [arXiv:1708.07962 \[hep-ex\]](#).
- [41] G. Aad et al. (ATLAS), (2022), [arXiv:2202.02039 \[hep-ex\]](#).
- [42] M. Bogomilov et al. (MICE), *Nature* **578**, 53 (2020), [arXiv:1907.08562 \[physics.acc-ph\]](#).
- [43] J. P. Delahaye, M. Diemoz, K. Long, B. Mansoulié, N. Pastrone, L. Rivkin, D. Schulte, A. Skrinsky, and A. Wulzer, (2019), [arXiv:1901.06150 \[physics.acc-ph\]](#).
- [44] N. Bartosik et al., *JINST* **15**, P05001 (2020), [arXiv:2001.04431 \[hep-ex\]](#).
- [45] J. A. Aguilar-Saavedra, *Nucl. Phys. B* **828**, 289 (2010), [arXiv:0905.2221 \[hep-ph\]](#).
- [46] F. del Aguila and J. A. Aguilar-Saavedra, *Nucl. Phys. B* **813**, 22 (2009), [arXiv:0808.2468 \[hep-ph\]](#).
- [47] M. S. Chanowitz and M. K. Gaillard, *Nucl. Phys. B* **261**, 379 (1985).
- [48] B. W. Lee, C. Quigg, and H. B. Thacker, *Phys. Rev. Lett.* **38**, 883 (1977).
- [49] R. Franceschini, T. Hambye, and A. Strumia, *Phys. Rev. D* **78**, 033002 (2008), [arXiv:0805.1613 \[hep-ph\]](#).
- [50] J. A. Casas and A. Ibarra, *Nucl. Phys. B* **618**, 171 (2001), [arXiv:hep-ph/0103065](#).
- [51] A. Atre, T. Han, S. Pascoli, and B. Zhang, *JHEP* **05**, 030 (2009), [arXiv:0901.3589 \[hep-ph\]](#).
- [52] P. Fileviez Perez, T. Han, and T. Li, *Phys. Rev. D* **80**, 073015 (2009), [arXiv:0907.4186 \[hep-ph\]](#).
- [53] C. Biggio, E. Fernandez-Martinez, M. Filaci, J. Hernandez-Garcia, and J. Lopez-Pavon, *JHEP* **05**, 022 (2020), [arXiv:1911.11790 \[hep-ph\]](#).
- [54] P. Fileviez Pérez and A. D. Plascencia, *Phys. Rev. D* **102**, 015010 (2020), [arXiv:2005.04235 \[hep-ph\]](#).
- [55] C. Han, T. Li, and C.-Y. Yao, *Phys. Rev. D* **104**, 015036 (2021), [arXiv:2103.03548 \[hep-ph\]](#).
- [56] I. Esteban, M. C. Gonzalez-Garcia, M. Maltoni, T. Schwetz, and A. Zhou, *JHEP* **09**, 178 (2020), [arXiv:2007.14792 \[hep-ph\]](#).

- [57] NuFIT v5.1, www.nu-fit.org (2021).
- [58] N. Aghanim et al. (Planck), *Astron. Astrophys.* **641**, A6 (2020), [Erratum: *Astron. Astrophys.* 652, C4 (2021)], [arXiv:1807.06209](https://arxiv.org/abs/1807.06209) [[astro-ph.CO](#)].
- [59] J. Alwall, R. Frederix, S. Frixione, V. Hirschi, F. Maltoni, O. Mattelaer, H. S. Shao, T. Stelzer, P. Torrielli, and M. Zaro, *JHEP* **07**, 079 (2014), [arXiv:1405.0301](https://arxiv.org/abs/1405.0301) [[hep-ph](#)].
- [60] T. Han, Y. Ma, and K. Xie, *Phys. Rev. D* **103**, L031301 (2021), [arXiv:2007.14300](https://arxiv.org/abs/2007.14300) [[hep-ph](#)].
- [61] H. Al Ali et al., (2021), [arXiv:2103.14043](https://arxiv.org/abs/2103.14043) [[hep-ph](#)].
- [62] R. Ruiz, A. Costantini, F. Maltoni, and O. Mattelaer, (2021), [arXiv:2111.02442](https://arxiv.org/abs/2111.02442) [[hep-ph](#)].
- [63] T. Sjöstrand, S. Ask, J. R. Christiansen, R. Corke, N. Desai, P. Ilten, S. Mrenna, S. Prestel, C. O. Rasmussen, and P. Z. Skands, *Comput. Phys. Commun.* **191**, 159 (2015), [arXiv:1410.3012](https://arxiv.org/abs/1410.3012) [[hep-ph](#)].
- [64] J. de Favereau, C. Delaere, P. Demin, A. Giammanco, V. Lemaître, A. Mertens, and M. Selvaggi (DELPHES 3), *JHEP* **02**, 057 (2014), [arXiv:1307.6346](https://arxiv.org/abs/1307.6346) [[hep-ex](#)].
- [65] M. Cacciari, G. P. Salam, and G. Soyez, *Eur. Phys. J. C* **72**, 1896 (2012), [arXiv:1111.6097](https://arxiv.org/abs/1111.6097) [[hep-ph](#)].